Optics and Lasers in Engineering 126 (2020) 105918

Contents lists available at ScienceDirect

Optics and Lasers in Engineering

journal homepage: www.elsevier.com/locate/optlaseng

Laser beam modulation with a fast focus tunable lens for speckle reduction in laser projection displays

Zequn Jian[a,b,1], Zhaomin Tong[a,b,1,*], Yifei Ma[a,b], Mei Wang[a,b], Suotang Jia[a,b], Xuyuan Chen[a,b,c]

[a] State Key Laboratory of Quantum Optics and Quantum Optics Devices, Institute of Laser Spectroscopy, Shanxi University, Wucheng Rd. 92, Taiyuan, Shanxi 030006, People's Republic of China

[b] Collaborative Innovation Center of Extreme Optics, Shanxi University, Taiyuan, Shanxi 030006, People's Republic of China

[c] Faculty of Technology and Maritime Sciences, Department of Micro- and Nanosystem Technology, University of Southeast Norway, Borre N-3184, Norway

ARTICLE INFO

Keywords:
Speckle reduction
Focus tunable lens
Angular diversity
Spatial diversity

ABSTRACT

We propose a laser speckle reduction method using a fast focus tunable lens (FTL). Different laser beams are generated after modulating the FTL. Thus, when the laser beams are used to illuminate a diffuser, various speckle images are obtained, and the summed speckle images yield a reduced speckle contrast ratio. To maximize the tuning range of the focal length of the FTL for efficient speckle reduction, the FTL operates in a resonant mode at the resonant frequency at 97 Hz. The effect of the change of the distance between the FTL and the diffuser on the efficiency of speckle reduction is investigated. Experimental results show that the lowest objective speckle contrast ratio is 0.05. After the application of this speckle reduction component in a laser projector, the subjective speckle contrast ratio is reduced from 0.16 to 0.09. In comparison with other speckle reduction methods, the method proposed in this study is simple and effective, and can be used in practice in laser projection displays.

1. Introduction

Lasers are preferred to be used as illumination light sources in displays owing to their good monochromaticity and directionality [1]. Compared with other display technologies, laser displays can provide wider color gamut, increased brightness, and increased optical efficiency [2]. One of the problems associated with the use of lasers in displays is the speckle effect, which is caused by the coherence property of laser manifested as strong grainy interferences when lights are scattered from an object with rough surfaces [3]. The existence of the laser speckle can seriously degrade image quality. Correspondingly, speckle reduction is required in laser displays. Speckle reduction can be achieved using wavelength [4–7], angular [7–9], and polarization diversities [10]. Other speckle reduction methods include the combination of a fast scanning micromirror and a multi-mode fiber [11,12], vibration of screens or diffusers [13–15], binary micro-mirror arrays [16,17], and dynamic deformable mirrors [18,19]. Among these speckle reduction techniques, most of them can effectively suppress speckle. However, some of these are expensive, complicated, or bulky, and hence unsuitable for practical laser display applications.

In this study, we propose a simple and effective laser speckle reduction method by introducing a fast focus tunable lens (FTL). Sinusoidal signals are used to drive the FTL, making the focal length of the FTL change between minimum and maximum values, thus realizing laser beam modulation. When the modulated laser beams are used to illuminate an object with rough surfaces, it produces different speckle patterns. Thus, speckle reduction can be achieved after summing these speckle patterns during the exposure time of the charge-coupled device (CCD) camera. Speckle contrast ratio C is used to characterize the speckle effect. The speckle contrast ratio C is defined as [20]

$$C = \frac{\sqrt{\langle I^2 \rangle - \langle I \rangle^2}}{\langle I \rangle} = \frac{\sigma_I}{\langle I \rangle}, \tag{1}$$

where $\langle I \rangle$ and σ_I represent the mean value and the standard deviation of light intensity, respectively. For fully developed speckles, the speckle contrast ratio equals one. It is reported that the human eye cannot detect the presence of speckle when the value of speckle contrast ratio is lower than 0.05 [11]. We can also use the number of the independent speckle patterns to evaluate the speckle contrast ratio. If N independent speckle patterns are summed together, the speckle contrast ratio C can be reduced from one to [20]

$$C = \frac{1}{\sqrt{N}}. \tag{2}$$

* Corresponding author at: Zhaomin Tong, State Key Laboratory of Quantum Optics and Quantum Optics Devices, Institute of Laser Spectroscopy, Shanxi University, Wucheng Rd. 92, Taiyuan, Shanxi 030006, People's Republic of China

E-mail address: zhaomin.tong@sxu.edu.cn (Z. Tong).

[1] Both authors contributed equally.

https://doi.org/10.1016/j.optlaseng.2019.105918

Received 23 May 2019; Received in revised form 26 September 2019; Accepted 24 October 2019

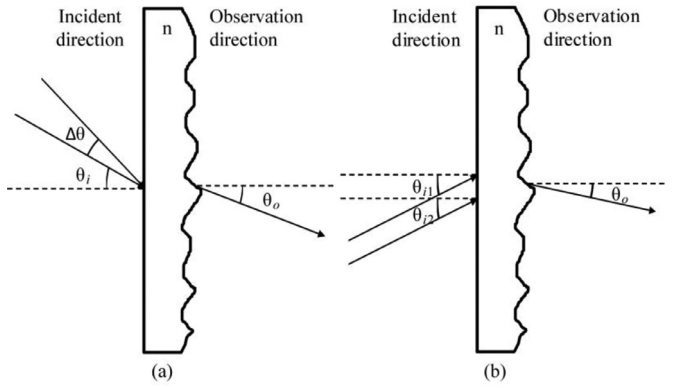

Fig. 1. Speckle reduction mechanisms evaluated in this study: (a) angular and (b) spatial diversities.

Figs. 1(a) and 1(b) schematically show the speckle reduction mechanisms that are partially based on the angle and spatial diversities. One spot on the diffuser is illuminated by two laser beams with the angles of incidence of θ_i and $\theta_i + \Delta\theta$. In this case, θ_o is the observation angle. We define a scattering vector $\vec{q}$ according to

$$\vec{q} = \vec{k}_o - \vec{k}_r = \vec{q}_t + \vec{q}_z, \tag{3}$$

where $\vec{k}_o$ and $\vec{k}_r$ are the observed and refracted k-vectors, respectively. Equivalently, $\vec{q}_z$ and $\vec{q}_t$ are the normal and the transverse components of the scattering vector $\vec{q}$, respectively.

The covariance of light intensity for the two laser beams at different angles of incidence on the diffuser shown in Fig. 1(a) can be written as [20]

$$|\mu_A(\vec{q}_1, \vec{q}_2)|^2 = |M_h(\Delta q_z)|^2 |\Phi(\Delta q_t)|^2, \tag{4}$$

where $|\mu_A(\vec{q}_1, \vec{q}_2)|^2$ is the covariance of the light intensity, $|M_h(\Delta q_z)|^2$ is the first-order characteristic function of the surface-height fluctuations, and $|\Phi(\Delta q_t)|^2$ is the translation of the speckle pattern when the incidence or observation angle is changed. Additionally, $\vec{q}_1$ and $\vec{q}_2$ are the scattering vectors, and Δq_z and Δq_t are the normal and the transverse components of the scattering vector difference $\Delta\vec{q} = \vec{q}_1 - \vec{q}_2$, respectively. Δq_z and Δq_t are given by [20]

$$\Delta q_z = \frac{2\pi}{\lambda}\left[\sqrt{n^2 - \sin^2(\theta_{i1} + \Delta\theta)} - \sqrt{n^2 - \sin^2\theta_{i1}}\right], \tag{5}$$

$$\Delta q_t = \frac{2\pi}{\lambda}\left[\sin(\theta_{i1} + \Delta\theta) - \sin\theta_{i1}\right]. \tag{6}$$

As the scattering vector difference $\Delta\vec{q}$ increases, the angle difference $\Delta\theta$ between vector $\vec{q}_1$ and $\vec{q}_2$ becomes larger, which makes the intensity covariance $|\mu_A(\vec{q}_1, \vec{q}_2)|^2$ smaller. Thus, the decoherence of the illuminating light source increases, and the speckle contrast ratio can be reduced [20]. Summation of the independent speckle patterns when the FTL works, yields the value of N (see Eq. (2)) according to

$$N = \frac{\Delta\theta}{\Delta\delta}, \tag{7}$$

where $\Delta\delta$ is the de-correlation angle which makes the two observed speckle patterns completely uncorrelated.

The speckle reduction mechanism owing to the spatial diversity is shown in Fig. 1(b). Two adjacent points on the diffuser are illuminated by two laser beams with the angles of incidence θ_{i1} and θ_{i2}. In this case θ_o is the angle of observation. When the distance between the adjacent points is smaller than the resolution of the imaging system, the speckle patterns will be averaged. When a moving diffuser is placed close to a smooth and transparent object, the phases of illumination of all the object points change as the diffuser moves. The intensity of the speckle on the image changes with the movement of the diffuser during the exposure time. The intensity captured by the detector is the summation of over many independent speckle patterns. The speckle contrast ratio C is given by [20]

$$C \approx \sqrt{\frac{\lambda z/D}{vT}}, \tag{8}$$

where $\lambda z/D$ is the image resolution cell on the object, and vT is the distance moved by the diffuser. The speckle contrast ratio is reduced as a function of the square root of the number of resolution widths on the object through which the diffuser had passed during its motion during the exposure time.

2. Characterization of the FTL

Fig. 2 schematically shows the working principle of the shape-changing FTL (EL-10-30-TC from Optotune). The FTL has a clear aperture of 10 mm and the response time is smaller than 2.5 ms. The FTL is composed of an electromagnetic actuator and an elastic polymer membrane filled with optical fluid [21]. When the electromagnetic actuator works to exert pressure on the container, more fluid fills the clear volume of the FTL, and the deflection of the FTL increases [22,23]. Therefore, the focal length of the FTL decreases. The maximum and minimum driving currents are 0 mA and 250 mA, respectively. The working frequency of the FTL ranges from 0 Hz to 1 kHz. The CW damage threshold of lens material is 10 kW/cm^2 for a wavelength of 1064 nm. Both the optical fluid and the membrane material are highly transparent in the range of 400–2500 nm and the transmission is 95.9% at the wavelength of 532 nm [22].

We have used a camera beam profiler (BC106N-VIS/M from Thorlabs) to calibrate the focal length of the FTL. Fig. 3 shows the relationship between the focal length of the FTL and the driving current. The minimum focal length is f_{min} = 44.5 mm and the maximum focal length is f_{max} = 160.5 mm.

To realize speckle reduction by generating different speckle images and summing them together during the detector integration period, alternating currents are used to drive the FTL to induce temporal-dependent changes of the focal length of the FTL. The tuning range of the focal length varies at different driving frequencies. When the frequency of the driving current equals the resonant frequency of the elastic polymer membrane, the strongest elastic polymer membrane vibration is realized, and the tuning range of the focal length is maximized largest [23–25]. Fig. 4 shows the experimental setup used to characterize the resonant frequency of the elastic polymer membrane.

As shown in Fig. 4, we have used a collimated multimode laser diode (L520P50 from Thorlabs) as the illumination light source. The central wavelength of the laser diode is λ = 520 nm. The driving current of the laser diode is 120 mA, and the working temperature of the laser diode is stabilized at 10 °C using a thermoelectric controller. The output power

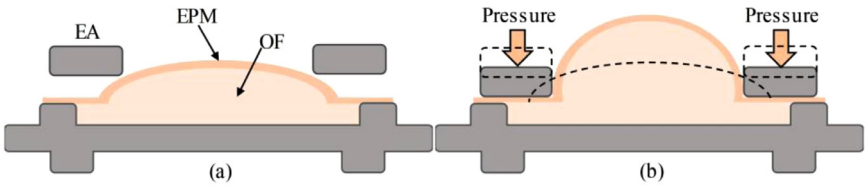

Fig. 2. Working principle of the FTL. (a) FTL before the application of pressure. (b) FTL after the application of pressure (EA: Electromagnetic actuator, EPM: Elastic polymer membrane, OF: Optical fluid).

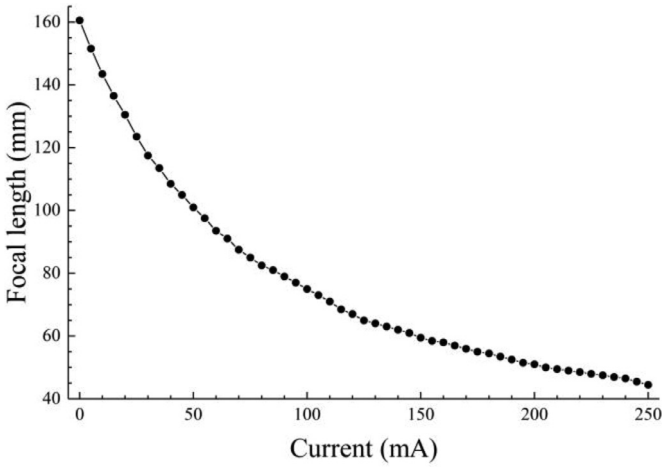

Fig. 3. Relationship between the focal length of the FTL and the driving current.

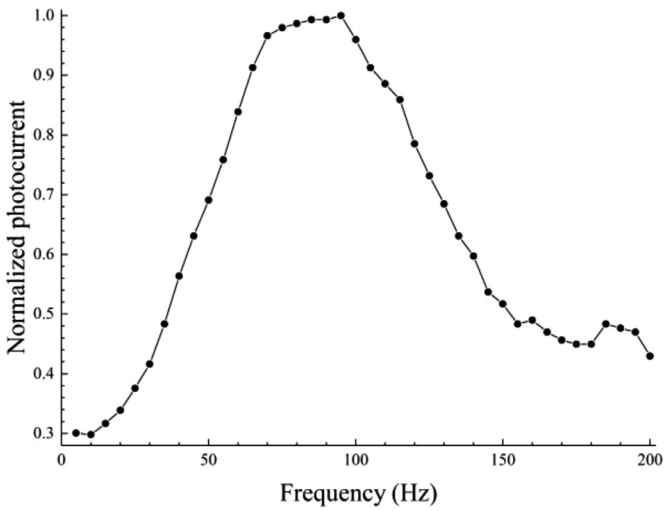

Fig. 5. Relationship between the normalized peak-to-peak photocurrent and the working frequency of the FTL.

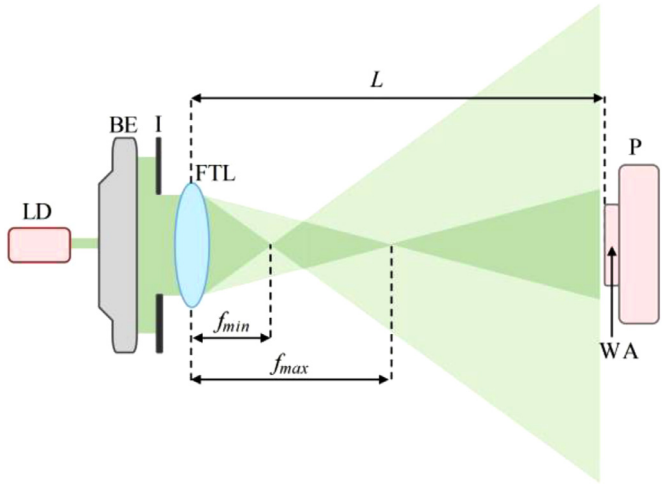

Fig. 4. Experimental setup used to characterize the resonant frequency of the elastic polymer membrane (LD: laser diode, BE: beam expander, I: iris, FTL: focal tunable lens, P: photodetector, WA: working area of the photodetector).

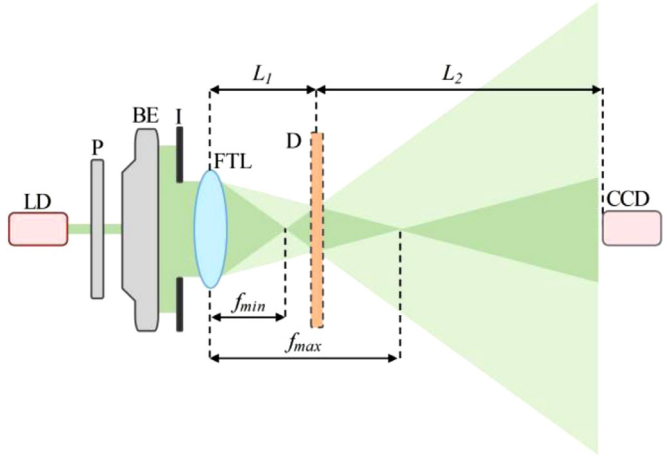

Fig. 6. Schematic of the optical path of the FTL in the case of sinusoidal signal modulation. The diffuser is placed at the position (the regions inside the dotted black lines) at which the beam diameter is the smallest (LD: laser diode, P: polarizer, BE: beam expander, I: iris, FTL: focal tunable lens, D: diffuser, CCD: charge-coupled device camera).

of the laser diode is 50 mW. A 20 × beam expander and circular iris (with a diameter of 8 mm) are introduced to magnify the laser beam and redefine the laser beam width, respectively. After the laser beam passes through the FTL, light intensity is measured by a photodetector (PDA36A from Thorlabs). The photodetector has a rectangular working area of 3.6 mm × 3.6 mm. The distance between the photodetector and the FTL is $L = 290$ mm, which is larger than the maximum focal length $f_{max} = 160.5$ mm of the FTL. The reason for the choice of this value of distance L is based on the fact that the photocurrent generated by the photodetector has a one-to-one relationship with the change of the focal length of the FTL in this situation. For example, when the driving current decreases from its peak to its valley value, the focal length of the FTL varies from the maximum value f_{max} to the minimum value f_{min}, and the number of photons captured by the working area of the photodetector decreases correspondingly. An oscilloscope (TBS 1052B from Tektronix) was used to measure the peak-to-peak photocurrent generated by the photodetector.

Fig. 5 shows the normalized peak-to-peak photocurrent measured by the oscilloscope when the driving frequency of the FTL was changed from 0 Hz to 200 Hz. As shown in Fig. 5, when the driving frequency of the FTL equals 97 Hz, the normalized peak-to-peak photocurrent has a maximum value. Therefore, we choose 97 Hz as the working frequency of the FTL to maximize the tuning range of the focal length of the FTL to achieve the most efficient speckle reduction.

3. Experiments and discussions

3.1. Speckle reduction in free-space propagation

Fig. 6 schematically shows the experimental setup for the speckle reduction measurement in free-space propagation using the FTL. Herein, a similar optical configuration was used to that shown in Fig. 4. A rotating polarizer is employed to control the laser beam intensity, and a 50 mm × 50 mm square diffuser (43–724 120-grit sandblasted glass from Edmund Optics) is placed after the FTL. During the experiment, the distance from the FTL and the diffuser L_1 is changed from 45 mm to 165 mm. Speckle patterns propagating in free-space are recorded by a CCD camera. The exposure time of the CCD camera is set to 30 ms, which is close to the time required by the human eyes to integrate the visual signal [20]. The CCD camera has a resolution of 1280 × 1024 pixels, and each pixel has a dimension of 5.2 μm × 5.2 μm. The brightness of the speckle images recorded by the CCD camera is modulated by the

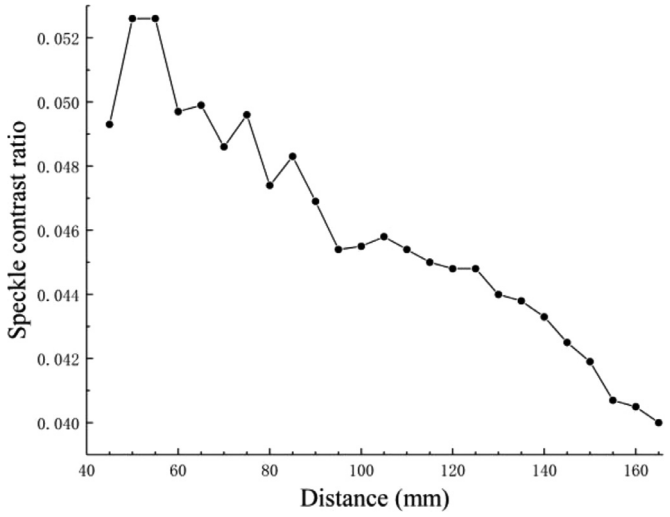

Fig. 7. Experimental results showing the variation of the speckle contrast ratio as a function of distance.

rotating polarizer to avoid overexposure and underexposure. The working frequency of the FTL equals its resonant frequency at 97 Hz. The diffuser and the CCD camera are mounted on a precision translation stage. Accordingly, the distance between the FTL and the diffuser can be accurately controlled. The distance from the diffuser and the CCD camera is constant with a value $L_2 = 260$ mm.

When the distance L_1 is changed, speckle images are captured by the CCD camera. Eq. (1) was used to calculate the speckle contrast ratio C. Fig. 7 shows the relationship between the distance L_1 and the speckle contrast ratio C when the FTL is working.

As shown in Fig. 7, when the distance L_1 becomes larger, the speckle contrast ratio exhibits sequential rising and falling edges. When the distance L_1 equals 55 mm, the speckle contrast ratio has a maximum value. The laser beam size on the diffuser changes by moving the diffuser, which alters the coherence properties of the laser beam which propagates on the diffuser. Accordingly, we have that [26]

$$\theta_{\mathrm{coh}} = \frac{\lambda}{\pi r_{di}}, \tag{9}$$

where the coherence divergence angle θ_{coh} depends on the beam radius r_{di} on the diffuser. The laser beams are captured by the CCD camera after propagating through the diffuser, and the size of the coherence area on the CCD camera is $A_{coh} = \pi(L_2 \tan\theta_{coh})^2$. Thus, the coherence area on the CCD camera is inversely proportional to the laser beam radius r_{di} of the diffuser. According to the geometrical optics principle, the various sizes of the laser beam on the diffuser exhibit a falling trend followed by a rising trend when the distance L_1 increases from 45 mm to 165 mm. The smallest size of the laser beam is 4.5 mm when the distance L_1 equals to 69.7 mm. Therefore, the coherence area on the CCD camera exhibits a rising trend followed by a falling trend as the distance L_1 increases. For small coherence area on the CCD camera, the sensor of the CCD camera cannot distinguish different speckle patterns in a single pixel. Thus, only the average value of the different speckle patterns will be recorded in this single pixel, which will lead to speckle reduction. Consequently, the speckle contrast ratio has a maximum value at $L_1 = 69.7$ mm owing to the spatial diversity. However, the speckle contrast ratio is maximized at $L_1 = 55$ mm, as shown in Fig. 7.

The radius of the laser beam on the diffuser is rapidly changed when the working frequency is 97 Hz. The movement of the laser beam during the CCD camera exposure time is equivalent to the moving diffuser mentioned in the introduction. The tuning range of the radius and the size of pixel of the CCD camera are equivalent to the movement distance vT and the image resolution cell on the object $\lambda z/D$, respectively. Therefore, the tuning range of the radius becomes inversely proportional to the speckle contrast ratio owing to the spatial diversity.

Thus, we define the direction of the incident beam on the diffuser as positive when the normal line rotates at the incident angle in the anticlockwise direction, and when the normal line rotates at the incident angle in the clockwise direction, the direction of incident beam on the diffuser is negative. When the distance L_1 becomes equal to f_{min}, the direction of the incident beam at every spot (expect the focal spot) on the diffuser has single direction (positive or negative). When the position of the distance L_1 is $\geq$ 69.7 mm, the incident beam has positive and negative directions at all the illuminated points on the diffuser. Therefore, the angular diversity increases as a function of the distance L_1 when it is $\leq$ 69.7 mm. The directional diversity has a constant value when the distance L_1 is $\geq$ 69.7 mm.

As shown in Fig. 7, the speckle contrast ratio is increased owing to the decrease of the size of the coherence area on the CCD camera when the distance L_1 is less than 55 mm. When the distance L_1 ranges between 55 mm and 69.7 mm, the angular diversity is the dominant speckle reduction mechanism. The speckle contrast ratio is decreased owing to the increased directional diversity. When the distance L_1 is $\geq$ 69.7 mm, the dominant speckle reduction mechanism is attributed to the spatial diversity. The speckle contrast ratio is decreased owing to the increased spatial diversity. Considering the problem of the optical power loss, we need to place the diffuser at the position where the beam diameter is the smallest to utilize light. Accordingly, we placed the diffuser at the distance $L_1 = 69.7$ mm. Figs. 8(a) and 8(b) show the speckle images before and after the speckle reduction when the distance $L_1 = 69.7$ mm. The speckle contrast ratios are 0.84 and 0.05 for Figs. 8(a) and 8(b), respectively.

3.2. Application in laser projection displays

Fig. 9 shows a simplified optical system exemplifying the application of this method in laser projection displays. The distance between the holographic diffuser and the FTL is 69.7 mm. The diffusion angle of

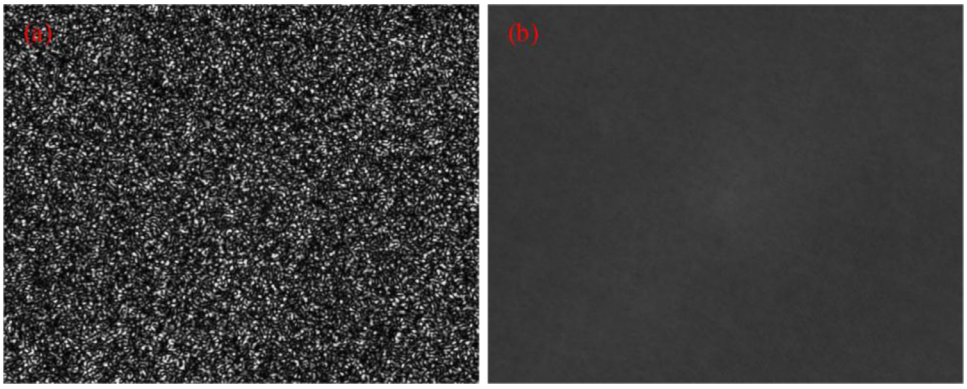

Fig. 8. Recorded speckle images using the CCD camera before (a) and after (b) the speckle reduction.

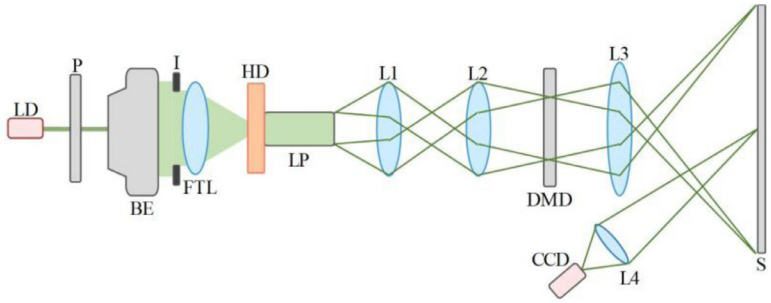

Fig. 9. Speckle measurement and reduction setup in laser projection displays (LD: laser diode, P: polarizer, BE: beam expander, I: iris, FTL: focal tunable lens, HD: holographic diffuser, LP: light pipe, L1: relay lens, L2: field lens, L3: projection lens, L4: imaging lens, DMD: digital micromirror device, CCD: charge-coupled device camera, S: screen).

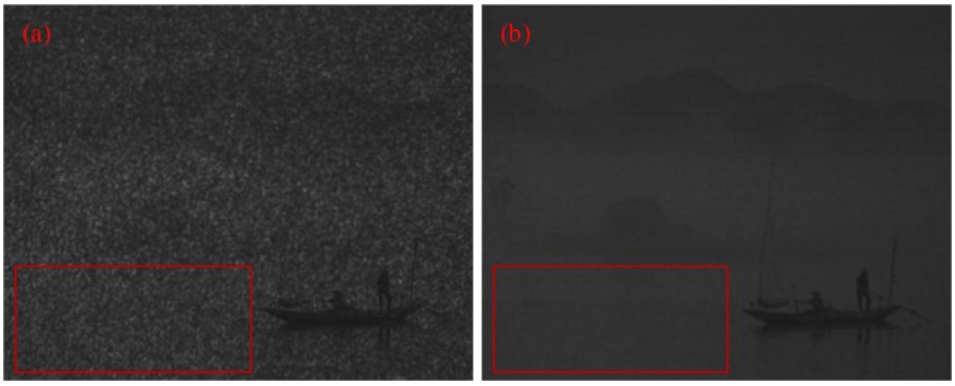

Fig. 10. Projected images on the screen in laser projection displays captured by the CCD camera before (a) and after (b) driving the FTL.

the holographic diffuser (47,994 from Edmund Optics) is 5°. The optical power loss of the holographic diffuser is 10.3%. A hollow light pipe is placed closely after the holographic diffuser. The light pipe is 20 mm long, where the internal surfaces of the light pipe are coated by highly reflective metal. The dimensions of the rectangular entrance surface and exit surface of the light pipe are both 5 mm × 6 mm. The dimension of the rectangular surface is larger than the laser beam diameter (4.5 mm) at this position. Therefore, the light pipe can collect all the scattered light from the holographic diffuser, and the optical power loss can be minimized. With the help of the combination of the holographic diffuser and the light pipe, the optical field is homogenized for uniform illumination. A relay lens and a field lens are used to transfer the optical field at the exit surface of the light pipe to a digital micromirror device (DMD). The image information generated by the DMD is projected onto a screen by a projection lens. The focal length and F-number of projection lens are 24 mm and 2.41, respectively. A CCD camera mounted with an imaging lens is used to capture the enlarged image on the screen. The material of the screen is soft polyvinyl chloride with metallic coatings. The focal length of the imaging lens is 35 mm, and the F-number is 4. The distance between the projection lens and the screen is 1000 mm. The distance between the CCD camera and the screen is 1600 mm. The exposure time of the CCD camera is set to 30 ms.

Fig. 10 shows the projected pictures captured by the CCD camera using the optical system shown in Fig. 9 before and after driving the FTL. Speckle contrast ratios are calculated by selecting areas with uniform brightness (the regions inside the solid red lines). After driving the FTL, the speckle contrast ratio is reduced from 0.16 to 0.09.

The speckle generated in the screen is the compound speckle, and consists of coarse and fine speckles. The coarse speckle pattern is created on the holographic diffuser before it propagates through the projection lens, and the fine speckle is generated on the screen. The speckle patterns captured by the CCD camera in the experiment of Fig. 6 are coarse speckle patterns. The speckle contrast ratio of the compound speckle is expressed as [20]

$$C = \sqrt{\frac{N + M + 1}{NM}}, \tag{10}$$

where N is the temporal degree of speckle reduction freedom. Effectively, this means that N independent speckle patterns are generated by the FTL during the exposure time of the CCD camera, and M is the spatial degree of the speckle reduction freedom. Accordingly, M is determined by the ratio of the resolution spot of the imaging lens of the CCD camera to the resolution spot of the projection lens of the laser projection displays. The dimensions of the resolution spot of the imaging and projection lenses are given by

$$L_i = \frac{1.22\lambda Z_i F\#_i}{f_i}, \tag{11}$$

$$L_p = \frac{1.22\lambda Z_p F\#_p}{f_p}, \tag{12}$$

where λ is the wavelength of the laser, Z_i and Z_p are the distances from the screen to the imaging lens and from the projection lens to the screen, respectively, $F\#_i$ and $F\#_p$ are the respective F-numbers of the imaging and the projection lenses, and f_i and f_p are the respective focal lengths of the imaging and the projection lenses. The spatial degree of speckle reduction freedom can consider as the number of resolution spots of the projection lens M that fit within the resolution spot of the imaging lens. This means that M resolution spots of the projection lens will be averaged within one resolution spot of the image lens. Accordingly, M can be expressed as

$$M = \frac{A_i}{A_p} = \left(\frac{L_i}{L_p}\right)^2 = \left(\frac{Z_i F_{\#i}/f_i}{Z_p F_{\#p}/f_p}\right)^2. \tag{13}$$

After the use of the FTL, the temporal degree of speckle reduction freedom N has increased. The large spatial degree of speckle reduction freedom M can be adjusted by choosing the optimal parameter of the projection displays. According to Eq. (13), the spatial degree of speckle reduction M equals 3.3. When the distance between the FTL and the holographic diffuser is 69.7 mm, the speckle contrast ratio is 0.05 after modulation by the FTL according to Eq. (2). Additionally, the temporal degree of speckle reduction freedom N is equal to 423, which is much larger than the spatial degree of the speckle reduction freedom M. For

very large N, the speckle contrast ratio $C = (1/M)^{1/2}$, which means that the speckle contrast ratio cannot be reduced to 0.05 owing to limited value of M. We can eliminate the coarse speckle on the holographic diffuser by the FTL, but we cannot eliminate the fine speckle generated on the screen. Thus, the compound speckle contrast ratio is large compared to the speckle contrast ratio in free-space propagation. Comparing with the moving diffuser mentioned in [27], the minimum subjective speckle contrast ratio obtained here is still too high. However, the FTL has the advantages such as simpler and more compact. After compounding the other independent speckle reduction mechanisms, for example, introducing K laser diodes as the illumination light sources, the speckle contrast ratio is expected to be reduced further to $0.09/K^{1/2}$ [20].

4. Conclusion

In conclusion, a laser speckle reduction method using the FTL has been proposed in this study based on which we have demonstrated laser speckle reduction in laser projection displays. Because the focal length of the FTL was changed when the FTL was driven by the sinusoidal signal, different angles of incidence were obtained when the modulated laser beam was used to illuminate the holographic diffuser, and the laser beam size on the holographic diffuser changed during the exposure time of the CCD camera. Therefore, the speckle reduction mechanisms were realized based on angular and spatial diversities. To achieve the most efficient speckle reduction, the FTL was driven using a resonant mode to maximize the vibration amplitude of the elastic polymer membrane and the tuning range of the focal length. In consideration of the dimension of the entrance surface of the light pipe, the holographic diffuser was placed at an optimized position to minimize the optical power loss. In these circumstances, the objective speckle contrast ratio was reduced to 0.05 in the case of free-space propagation, and the subjective speckle contrast ratio was reduced to 0.09 in the case of the laser projection system. In comparison with other speckle reduction methods, the method proposed in this study is simple and effective, and can be used in practice in laser projection displays.

Declaration of Competing Interest

None.

Acknowledgments

This research was supported by the National Key Research and Development Program of China (2016YFB0401903), the Key Research and Development Program of Shanxi Province for International Cooperation (201703D421015), the Changjiang Scholars and Innovative Research Team in University of Ministry of Education of China (IRT_17R70), the State Key Program of National Natural Science of China (11434007), the 111 project (D18001), and the Fund for Shanxi “1331 Project” Key Subjects Construction.

References

[1] Svelto O, Hanna DC. Principles of lasers. Plenum Press 1998:8–11.
[2] Chellappan KV, Erden E, Urey H. Laser-based displays: a review. Appl. Opt. 2010;49(25):F79–98.
[3] Akram MN, Chen X. Speckle reduction methods in laser-based picture projectors. Opt. Rev. 2016;23(1):108–20.
[4] Yu NE, Choi JW, Kang H, Ko DK, Fu SH, Liou JW, Kung AH, Choi HJ, Kim BJ, Cha M, Peng LH. Speckle noise reduction on a laser projection display via a broadband green light source. Opt. Express 2014;22(3):3547–56.
[5] Yilmazlar I, Sabuncu M. Speckle noise reduction based on induced mode hopping in a semiconductor laser diode by drive current modulation. Opt. Laser Technol. 2015;73:19–22.
[6] Yilmazlar I, Sabuncu M. Implementation of a current drive modulator for effective speckle suppression in a laser projection system. IEEE Photonics J. 2015;7(5):1–6.
[7] Tran TTK, Ø Svensen, Chen X, Akram MN. Speckle reduction in laser projection displays through angle and wavelength diversity. Appl. Optics 2016;55(6):1267–74.
[8] Wang Y, Meng P, Wang D, Rong L, Panezai S. Speckle noise suppression in digital holography by angular diversity with phase-only spatial light modulator. Opt. Express 2013;21(17):19568–78.
[9] Mehta DS, Naik DN, Singh RK, Takeda M. Laser speckle reduction by multimode optical fiber bundle with combined temporal, spatial, and angular diversity. Appl Optics 2012;51(12):1894–904.
[10] Trisnadi JI. Speckle contrast reduction in laser projection displays. Proc. SPIE 2002:131–8.
[11] Akram MN, Tong Z, Ouyang G, Chen X, Kartashov V. Laser speckle reduction due to spatial and angular diversity introduced by fast scanning micromirror. Appl. Optics 2010;49(17):3297–304.
[12] Tong Z, Shen W, Song S, Cheng W, Cai Z, Ma Y, Wei L, Ma W, Xiao L, Jia S, Chen X. Combination of micro-scanning mirrors and multi-mode fibers for speckle reduction in high lumen laser projector applications. Opt. Express 2017;25(4):3795–804.
[13] Tu SY, Lin HY, Lin MC. Efficient speckle reduction for a laser illuminating on a micro-vibrated paper screen. Appl. Optics 2014;53(22):E38–46.
[14] Pan JW, Shih CH. Speckle reduction and maintaining contrast in a laser pico-projector using a vibrating symmetric diffuser. Opt. Express 2014;22(6):6464–77.
[15] Shin SC, Yoo SS, Lee SY, Park C, Park S, Kwon JW, Lee S. Removal of hot spot speckle on laser projection screen using both the running screen and the rotating diffuser. Displays 2006;27(3):91–6.
[16] Tong Z, Chen X. Laser speckle reduction by using a binary micro mirror array (BMMA): theory and design. In: 2011 International Conference on Optical MEMS and Nanophotonics (OMN); 2011. p. 195–6.
[17] Tong Z, Principle Chen X. design and fabrication of a passive binary micro-mirror array (BMMA) for speckle reduction in grating light valve (GLV) based laser projection displays. Sensor Actuat A-PHYS 2014;210:209–16.
[18] Tran TKT, Chen X, Ø Svensen, Akram M N. Speckle reduction in laser projection using a dynamic deformable mirror. Opt. Express 2014;22(9):11152–66.
[19] Almoro PF, Glückstad J, Hanson SG. Single-plane multiple speckle pattern phase retrieval using a deformable mirror. Opt. Express 2010;18(18):19304–13.
[20] Goodman JW. Speckle phenomena in optics: theory and applications. Englewood. Colorado, USA: Roberts and Company Publishers; 2006.
[21] Blum M, Büeler M, Grätzel C, Aschwanden M. Compact optical design solutions using focus tunable lenses. Proc SPIE 2011;8167:81670W.
[22] <https://www.optotune.com/images/products/Optotune%20EL-10-30.pdf>.
[23] Casutt S, Bueeler M, Blum M, Aschwanden M. Fast and precise continuous focusing with focus tunable lenses. Proc. SPIE 2014;8982:89820Y.
[24] Gutierrez RH, Laura PAA, Bambill DV, Jederlinic VA, Hodges DH. Axisymmetric vibrations of solid circular and annular membranes with continuously varying density. J. Sound VIB 1998;212(4):611–22.
[25] Prokopczuk K, Rozwadowski K, Starzyńska MDA, Domański AW. Optical fiber sensor for membrane submicrometer vibration measurement. Appl. Optics 2014;53(26):6051–7.
[26] Mandel L, Wolf E. Optical coherence and quantum optics. Cambridge university press; 1995.
[27] Kubota S, Goodman JW. Very efficient speckle contrast reduction realized by moving diffuser device. Appl. optics 2010;49(23):4385–91.